Short communication

NiO/YSZ nanocomposite particles synthesized via co-precipitation method for electrochemically active Ni/YSZ anode

Kazuyoshi Sato *, Go Okamoto, Makio Naito, Hiroya Abe

Joining and Welding Research Institute, Osaka University, 11-1 Mihogaoka, Ibaraki, Osaka 567-0047, Japan

ABSTRACT

NiO/YSZ composite particles were synthesized via a co-precipitation of hydroxides. We investigated the effect of pH on the morphology of the composite particles, as well as on the microstructure and the electrochemical property of the Ni/YSZ anode. The particles synthesized at pH 10 involved aggregated composites and large NiO. The particles resulted in coarse and inhomogeneous anode microstructure and moderate area specific resistance (ASR) as $0.57\,\Omega\,cm^2$ at $800\,°C$ under open circuit voltage (OCV). Contrarily, nano-sized composite particles were successfully synthesized at pH 13. The particles provided fine as well as homogeneous porous structure with the grain size in the range 200–400 nm and low ASR as $0.36\,\Omega\,cm^2$ at $800\,°C$ under OCV.

© 2008 Elsevier B.V. All rights reserved.

1. Introduction

Nickel/yttria stabilized zirconia (Ni/YSZ) cermet is the promising anode material of solid oxide fuel cells (SOFCs). Since electrochemical performance of the Ni/YSZ anode strongly depends on the microstructure [1,2] considerable efforts have been made for the precise control of the microstructure to accelerate the hydrogen oxidation reaction [3–5]. Previous fundamental studies revealed that the hydrogen oxidation occurs at triple phase boundary (TPB) where Ni, YSZ and pore phases meet [6,7]. Detailed electrochemical investigations indicated that the dominant rate limiting steps in the Ni/YSZ anode involved dissociative adsorption of hydrogen molecules, diffusion of the hydrogen atoms on Ni surface moving toward the TPB, and the charge transfer reaction at the TPB [8,9]. Finer microstructure with uniform arrangement of Ni, YSZ and pore phases would be beneficial to decrease their contributions to the reaction rates, resulting in better electrochemical performance of the anode.

It had been widely accepted that the prefabrication of NiO/YSZ composite particles and their three-dimensional assembling are effective way to fabricate such anode microstructure [10–12]. A variety of methods such as spray pyrolysis [10], mechanical milling [11], and gel combustion [12] had been proposed for synthesis of the composite particles.

Theoretically, build-up process involving spray pyrolysis and gel combustion has the advantage in production of homogeneous multi-component and composite particles compared with break-down process involving mechanical milling. However, in common sense, the process have disadvantage in production cost. Although co-precipitation is categorized in build-up process, the method can provide high quality products with lower cost than other build-up processes. Thus the method is a promising candidate for production of NiO/YSZ composite particles and resultant fine Ni/YSZ anode microstructure. Theoretically, the method can provide fine and homogeneous composite structure, however the grain size was still around 1 μm or more in state-of-the-art Ni/YSZ anode derived from the NiO/YSZ composite particles synthesized by the method [13–15].

In this study, we report the synthesis of nano-sized NiO/YSZ composite particles via a co-precipitation of hydroxides in the highly basic solution (pH 13). We discussed effect of pH on the morphology of the composite particles from the view point of nucleation and growth behaviors of hydroxides in the solution. The composite particles provided not only fine but also homogeneous porous structure of the Ni/YSZ anode. Grain size of the anode was in the range 200–400 nm. The anode exhibited low area specific resistance (ASR) as $0.36\,\Omega\,cm^2$ at $800\,°C$.

2. Solubility curves of metal hydroxides

Understanding the precipitation behavior of the precursor from the solubility curves for precise morphology control of the composite particles is of prime importance. The precipitation of metal

---

* Corresponding author. Tel.: +81 668 79 4370; fax: +81 668 79 4370.
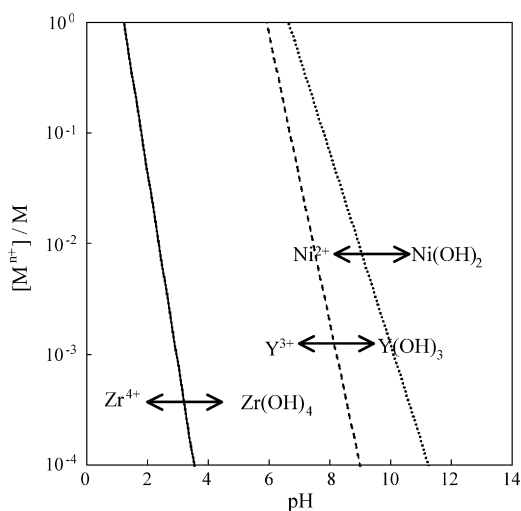 *E-mail address:* k-sato@jwri.osaka-u.ac.jp (K. Sato).

Fig. 1. Solubility curves of Zr(OH)$_4$, Y(OH)$_3$ and Ni(OH)$_2$ at 25 °C.

hydroxide M(OH)$_n$ can be described as

$$M^{n+} + n(OH)^- \rightarrow M(OH)_n \tag{1}$$

where n is the valence of metal ions in the solution. The solubility product K_{SP} of M(OH)$_n$ is

$$K_{SP} = [M^{n+}][OH^-]^n \tag{2}$$

$$\log K_{SP} = \log[M^{n+}] + n \log[OH^-] \tag{3}$$

$[M^{n+}]$ and $[OH^-]$ were the mole concentration of M^{n+} and OH^- in the solution, respectively. The ionic product of water at 25 °C under the ambient pressure was 10^{-14} M^2

$$-\log[H^+] - \log[OH^-] = pH + pOH = 14 \tag{4}$$

Therefore, Eq. (3) can be described as follows

$$\log K_{SP} = \log[M^{n+}] - 14n - n \log[H^+] \tag{5}$$

$$\log[M^{n+}] = -\log K_{SP} + 14n - n\,pH \tag{6}$$

$\log K_{SP}$ can be found in the literatures [16,17]. Fig. 1 shows the solubility curves of Zr(OH)$_4$, Y(OH)$_3$ and Ni(OH)$_2$ as the function of pH. M(OH)$_n$ precipitates, when pH of the solution exceeded the solubility curves. This figure indicated that Zr(OH)$_4$ start to precipitate prior to Y(OH)$_3$ and Ni(OH)$_2$, and almost finish at pH 4, then other hydroxides start to precipitate. Thus it would be difficult to synthesize nano-sized NiO/YSZ composite particles using a conventional co-precipitation condition, in which pH of the solution containing constituent metal ions increased step by step by adding some basic solution. To minimize the inhomogeneity, pH of the solution should be kept constant.

3. Experimental procedure

Fig. 2 shows scheme of the synthesis of NiO/YSZ composite particles. Mass fraction of NiO in the composite particles was chosen as 0.656. The mass fraction corresponds to the volume fraction of Ni in the Ni/YSZ anode as 0.5.

All of the reagents were purchased from Kanto Chemical. Co. Ltd, Japan. ZrOCl$_2$·8H$_2$O, Y(NO$_3$)$_3$·6H$_2$O and Ni(NO$_3$)$_2$·6H$_2$O were used as metal ion sources. These were dissolved into deionized water to prepare the source solution with the total metal ion concentration of 0.2 M. The solution was added dropwise into the concentrated NaOH solution to make the precipitates. The precipitation was conducted at pH 10 and pH 13. During the precipitation, extra NaOH solution was added simultaneously to keep pH value constant. The
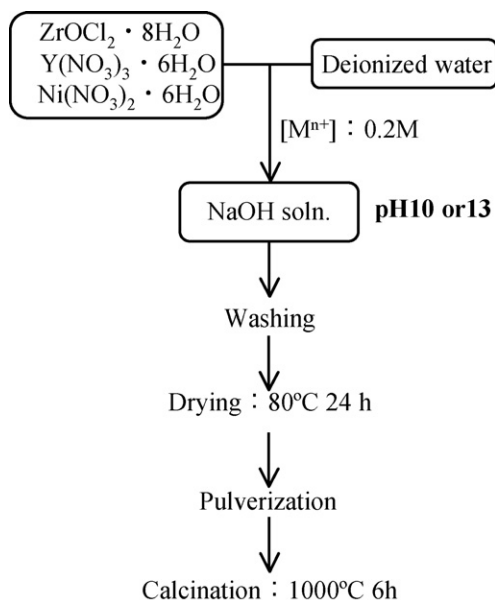

Fig. 2. Scheme of the synthesis of NiO/YSZ composite particles.

precipitates were washed by water four times and then by ethanol once. Then they were dried in an oven at 80 °C for 24 h. The dried precipitates were pulverized by alumina mortar and pestle and then calcined at 1000 °C for 6 h to obtain the NiO/YSZ composite particles.

Electrolyte supported cell was employed. First, fully dense YSZ electrolyte with the thickness of 300 μm and the diameter of 13 mm was fabricated by conventional tape casting followed by sintering at 1350 °C for 2 h. Then the anode was fabricated by screen printing of the paste consisting of the NiO/YSZ composite particles and polyethylene glycol followed by sintering at 1300 °C for 2 h. Finally, the cathode was fabricated by screen printing of the La$_{0.8}$Sr$_{0.2}$MnO$_3$ paste and subsequent sintering at 1100 °C for 2 h.

Three electrode-four leads configuration was applied for the electrochemical performance testing. The cell was fixed between alumina tubes with a glass sealant. Pt mesh was placed on both the cathode and the anode as Current collector. Pt wire was attached on circumference of the electrolyte as the reference electrode. Pt paste was applied on the reference electrode to improve the electric contact. The cell was heated up to 900 °C to soften the glass sealant for gas tightening. During the process, nitrogen was supplied for the anode and dry air was supplied for the cathode and the reference electrode with the flow rate of 0.05 l min^{-1}. After the temperature was reduced to 800 °C, anode gas atmosphere was changed from nitrogen to wet hydrogen containing 3 vol.% H$_2$O with the flow rate of 0.05 l min^{-1}. At this stage NiO was reduced into Ni. Electrochemical performance of the Ni/YSZ anode was examined by area specific resistance (ASR) measured by electrochemical impedance spectroscopy (EIS). The impedance spectra were recorded by frequency response analyzer with potentiostat (Parstat 2263, Princeton Applied Research, TN). The testing was conducted at the frequency range 0.1–10^5 Hz under the open circuit voltage (OCV) with applied amplitude of 20 mV.

Specific surface area (SSA) of the NiO/YSZ composite particles was measured by the nitrogen gas adsorption method. Microstructure of the NiO/YSZ composite particles and the Ni/YSZ anode was observed by scanning electron microscopy (SEM; ERA-8800FE, Eloinics, Japan).
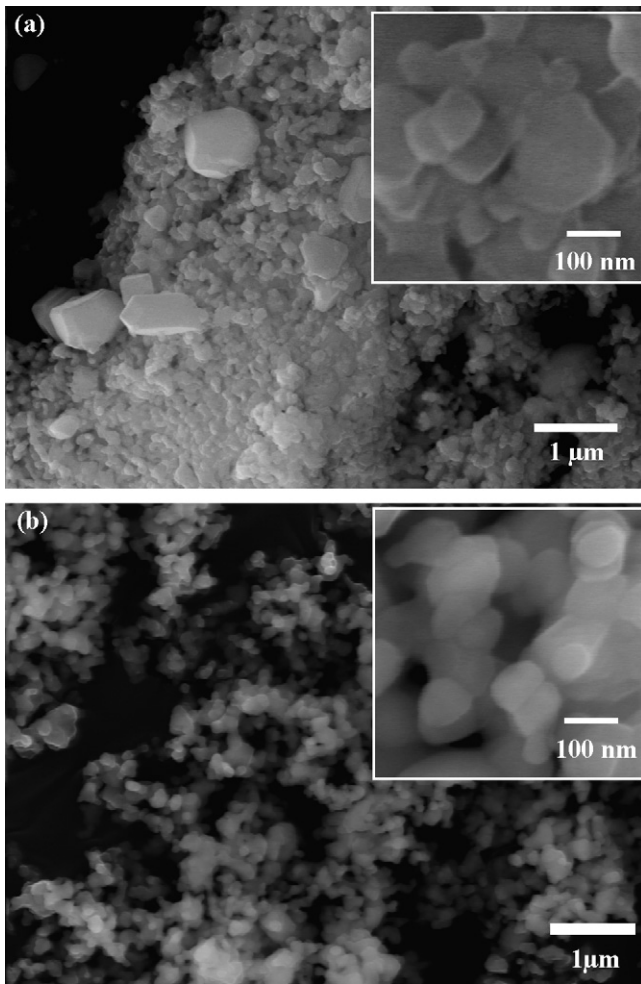
Fig. 3. SEM micrographs of the NiO/YSZ composite particles synthesized at (a) pH 10 and (b) pH 13.

Fig. 4. SEM micrographs of the Ni/YSZ anodes derived from the composite particles synthesized at (a) pH 10 and (b) pH 13 after the electrochemical testing.

4. Results and discussion

Microstructure of the NiO/YSZ composite particles drastically changed depending on pH of the solution. Fig. 3(a) shows SEM micrograph of the NiO/YSZ composite particles synthesized at pH 10. SSA of the composite particles was $5.3\,m^2\,m^{-1}$. The composite particles consisted of aggregated particles with the size 100–200 nm (see inset of Fig. 3(a)). Large particles in the range 0.5–1 µm were frequently observed. The spot analysis by energy dispersive X-ray spectroscopy (EDS) revealed that these large particles were NiO. Fig. 3(b) shows SEM micrograph of the composite particles synthesized at pH 13. SSA of the composite particles was $4.6\,m^2\,m^{-1}$. The micrograph indicated successful synthesis of nano-sized NiO/YSZ composite particles. The particle had fine as well as uniform size. The primary particle size appeared to be <100 nm (see inset of Fig. 3(b)).

The clear difference of the microstructure depending on pH of the solution might be attributed to difference of precipitation and growth behaviors of the hydroxides. The followings were expected with increasing pH

1. The size of precipitates decreases, since the number density of nuclei increases.
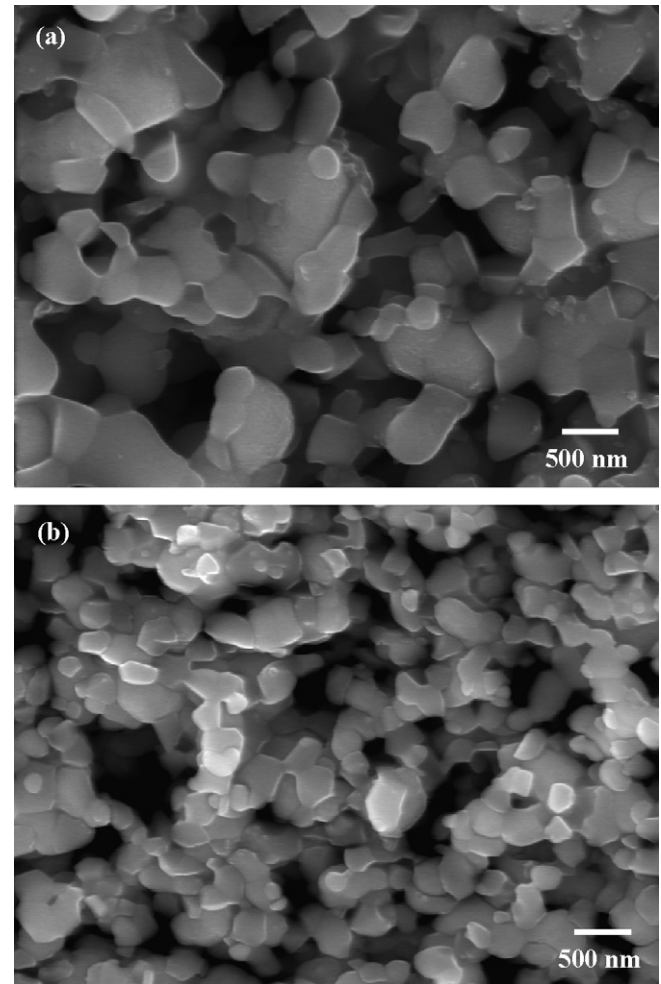2. The difference of precipitation rate between the hydroxides may decrease.

3. Ostwald ripening is suppressed, since higher pH can stabilize finer precipitates from the dissolution.

As a consequence, finer hydroxide phases with more uniform distribution can be obtained at pH 13 than pH 10. The uniformly distributed NiO and YSZ phases suppressed the grain growth each other during the subsequent calcination step [11], resulting in successful synthesis of nano-sized NiO/YSZ composite particles at pH 13.

Fig. 4 shows the microstructure of the Ni/YSZ anodes after the performance testing. The microstructures reflected that of the NiO/YSZ composite particles. Nonuniform microstructure was observed in the anode fabricated from the NiO/YSZ composite particles synthesized at pH 10. The grain size was broad and was in the range 200 nm–1 µm. Broad size distribution of the composite particles as shown in Fig. 3(a) would provide driving force for grain growth. Thus coarse and nonuniform microstructure was observed in the anode. Contrarily, fine as well as uniform porous structure was observed in the anode fabricated from the composite particles synthesized at pH 13. The grain size was in the range 200–400 nm. The uniform as well as fine microstructure would be attributed to the narrow size distribution of the particles as shown in Fig. 3(b) and uniform distribution of NiO and YSZ phases. The anode microstructure anticipated high electrochemical performance.

Fig. 5 shows EIS spectra and Bode (phase) diagram of the Ni/YSZ anodes recorded at 800 °C. Area specific resistance (ASR) of the anodes derived from the composite particles synthesized
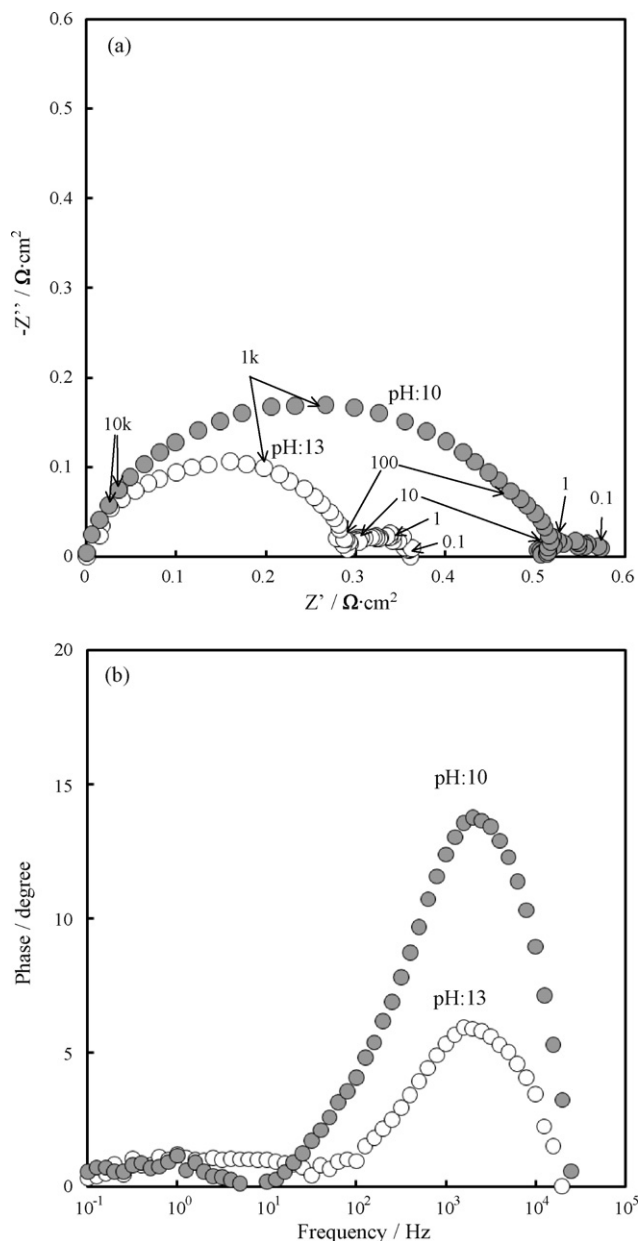
Fig. 5. (a) Electrochemical impedance spectra and (b) Bode (phase) diagram of the anode derived from the NiO/YSZ composite particles synthesized at pH 10 and pH 13. The measurement was carried out at 800 °C under OCV.

at pH 10 and pH 13 was 0.57 and 0.36 Ω cm², respectively. These results indicated that the performance is strongly depends on the microstructure of the anode, namely on the synthesis condition of the NiO/YSZ composite particles. Impedance arc appeared over the wide frequency range for both anodes. It was proposed that the low frequency arc (0.1–10 Hz) was attributed to gas conversion [18], the medium frequency arc (10 Hz–1 kHz) was attributed to gas diffusion [19], and high frequency arc (1–50 kHz) would be related to gas–solid (desorption, adsorption, dissociation) [2] or solid–solid reaction (surface diffusion, ion transfer across the double layer) [20] for hydrogen oxidation in Ni/YSZ anode.

Bode diagram revealed that clear difference appeared at high frequency range. Based on the proposed rate determining mechanisms as mentioned above, the difference would be mainly attributed to the gas–solid and/or solid–solid reaction. The result indicated that the finer grains of the anode fabricated from the NiO/YSZ composite particles synthesized at pH 13 would contribute to extend the adsorption sites of hydrogen molecules, reduce the average diffusion path length of hydrogen atom from adsorption site to the TPB, and enlarge the TPB length, resulting in lower ASR at high frequency range. The difference in impedance spectra was also observed at medium frequency range. This would be attributed to difference in gas diffusion property related to the microstructure such as pore size, total porosity, and tortuosity of the pore channels.

In the present study, we used NaOH as precipitation agent. Since sodium may reduce long-term stability of the anode [21], complete removal of sodium or application of alkaline free precipitation agent might be a technical issue for application of this method. The long-term stability of this anode will be reported elsewhere.

5. Conclusions

We successfully synthesized nano-sized NiO/YSZ composite particles via a co-precipitation of constituent metal hydroxides under highly basic solution. The composite particles also provided fine as well as homogeneous porous structure of the Ni/YSZ anode. The anode with finer microstructure exhibited low ASR due to decreased contribution of gas–solid and/or solid–solid reactions.

Acknowledgement

References

[1] M. Brown, S. Primdahl, M. Mogensen, J. Electrochem. Soc. 147 (2000) 475–485.
[2] S. Primdahl, M. Mogensen, J. Electrochem. Soc. 144 (1997) 3409–3419.
[3] T. Kawada, N. Sakai, H. Yokokawa, M. Dokiya, M. Mori, T. Iwata, J. Electrochem. Soc. 137 (1990) 3042–3047.
[4] S.P. Jiang, Y.Y. Duan, J.G. Love, J. Electrochem. Soc. 149 (2002) A1175–A1183.
[5] S.P. Jiang, S. Zhang, Y.D. Zhen, W. Wang, J. Am. Ceram. Soc. 88 (2005) 1779–1785.
[6] J. Mizusaki, H. Tagawa, T. Saito, K. Kamitani, T. Takagi, T. Hikita, M. Ippommatsu, S. Nakagawa, K. Hasgimoto, J. Electrochem. Soc. 141 (1994) 2129–2134.
[7] A. Bieberle, L.P. Meier, L.J. Gauckler, J. Electrochem. Soc. 148 (2001) A646–A656.
[8] S.P. Jiang, S.P.S. Badwal, J. Electrochem. Soc. 144 (1997) 3777–3784.
[9] S.P. Jiang, Y. Ramprakash, Solid State Ionics 122 (1999) 211–222.
[10] T. Fukui, S. Ohara, M. Naito, K. Nogi, J. Power Sources 110 (2002) 91–95.
[11] T. Fukui, K. Murata, S. Ohara, H. Abe, M. Naito, K. Nogi, J. Power Sources 125 (2004) 17–21.
[12] S.-D. Kim, H. Moon, S.-H. Hyun, J. Moon, J. Kim, H.-W. Lee, J. Power Sources 163 (2006) 392–397.
[13] S. Mosch, N. Trofimenko, M. Kusnezoff, T. Betz, M. Kellner, Solid State Ionics 179 (2008) 1606–1610.
[14] M. Marinšek, K. Zupan, J. Maček, J. Power Sources 86 (2000) 383–389.
[15] C.M. Grgicak, R.G. Green, W.-F. Du, J.B. Giorgi, J. Am. Ceram. Soc. 88 (2005) 3081–3087.
[16] L.G. Sillén, A.E. Martell, Stability Constants of Metal-Ion Complexes, Chemical Society, London, No. 17 (1964) and No. 25 (1971).
[17] W. Feitknecht, P. Scindler, Pure Appl. Chem. 6 (1963) 130–199.
[18] S. Primdahl, M. Mogensen, J. Electrochem. Soc. 145 (1998) 2431–2436.
[19] S. Primdahl, M. Mogensen, J. Electrochem. Soc. 146 (1999) 2827–2833.
[20] S. Primdahl, Ph D Thesis, Risø National Laboratory, Denmark, 1999.
[21] Y.L. Liu, S. Primdahl, M. Mogensen, Solid State Ionics 161 (2003) 1–10.